49th AIAA Aerospace Sciences Meeting including the New Horizons Forum and Aerospace Exposition
4 - 7 January 2011, Orlando, Florida

Wing Section Thickness and Camber Allocation for Conceptual and Preliminary Aircraft Design

Arvin Shajanian[i]
Northrop Grumman Aerospace Systems

Timothy Takahashi[ii]
Santa Clara University

Brian German[iii]
Georgia Institute of Technology

Matthew Daskilewicz[iv]
Georgia Institute of Technology

Shane Donovan[v]
Northrop Grumman Aerospace Systems

Allocating a wing section thickness and camber for a given aircraft wing configuration is an essential task that has significant impacts across several engineering disciplines. This provided the motivation to develop a method to allocate wing section thickness and camber for a desired critical Mach number and required section lift coefficient. Various airfoil families were analyzed using a potential flow code to observe trends in section lift coefficient and critical Mach number. A method to allocate wing section thickness and camber for a given critical Mach number and desired section lift coefficient was developed for each of these families of airfoils. The method was designed to be rapidly repeatable so that it can easily be applied to other airfoil families, particularly non-conventional or custom airfoils.

Nomenclature

α	=	angle of attack
AR	=	wing aspect ratio
C_D	=	drag coefficient
C_l	=	wing section lift coefficient
$C_{l_{Design}}$	=	airfoil design lift coefficient
C_p^*	=	critical pressure coefficient
$C_{p_{\min}}$	=	minimum pressure coefficient
γ	=	gas specific heat ratio

[i] Engineer, Aerodynamic Design and Analysis, Northrop Grumman Aerospace Systems, El Segundo, CA, Professional Member AIAA.
[ii] Formerly Engineer V, Configuration and Integration Department, Multi-Disciplinary Analysis and Optimization (MDAO) Project Manager, Northrop Grumman Aerospace Systems, El Segundo, CA, Associate Fellow AIAA.
[iii] Assistant Professor, Daniel Guggenheim School of Aerospace Engineering, Georgia Institute of Technology, Senior Member AIAA.
[iv] Graduate Research Assistant, Daniel Guggenheim School of Aerospace Engineering, Georgia Institute of Technology, Student Member AIAA.
[v] Engineer, Aerodynamic Performance, Northrop Grumman Aerospace Systems, El Segundo, CA, Professional Member AIAA.

k	=	Korn equation technology factor
M	=	Mach number
M_{cr}	=	critical Mach number
M_{DD}	=	drag divergence Mach number
t/c	=	wing section thickness to chord ratio

I. Introduction

In conceptual and preliminary aircraft design, properly allocating wing thickness is one of the most critical responsibilities of the aerodynamicist and aircraft designer. Wing thickness directly and strongly influences several other design variables and requirements, including the maximum operating Mach number, aerodynamic lift and drag, the structural architecture of the wing, the available fuel volume in the wing, and the selection of a propulsion system. Improper allocation of wing thickness in the early design phases can result in an aircraft configuration that cannot meet its original design goals. For example, the aircraft may lack the fuel volume to achieve its payload-range target if not enough thickness is allocated, or it might not be able to achieve the desired cruise Mach number if too much thickness is allocated. With a parameter that is needed to be defined at such early phases of an aircraft's design that has such great impacts on overall aircraft performance measures, significant efforts should be focused on properly allocating wing thickness in the conceptual and preliminary design phases.

A typical approach to allocating wing thickness is to allocate a wing thickness to achieve a required maximum Mach number. If a wing design can achieve a desired maximum Mach number, then other aircraft design variables, such as fuel volume, drag, and structural weight, can be assessed for adequacy based on this configuration. Hence, the design problem of allocating wing thickness becomes a matter of first properly allocating a wing thickness to achieve a required maximum Mach number.

If a required maximum Mach number and a design lift coefficient are known, for a given airfoil section, a proper thickness can be allocated using existing methods. However, these methods are limited in their applicable range of airfoil types and associated wing geometries.

In general the wing geometry parameters that affect the critical Mach number are thickness, aspect ratio, taper ratio, and sweep angle. In addition to the wing geometry parameters, the airfoil sections of a wing also affect the critical Mach number. The characteristics of the airfoil that affect critical Mach number are the camber line and the thickness form of the airfoil. Therefore, to properly allocate wing thickness, the designer must be able to predict the effects on critical Mach number of wing thickness, aspect ratio, taper ratio, sweep angle, airfoil camber line, and airfoil thickness form.

Previous efforts, as described in *Zero Lift Drag and Drag Divergence Prediction for Finite Wings in Aircraft Design*[1], developed a method to calculate form factor and critical Mach number for a given wing from streamwise wing pressure coefficients computed using a potential flow code. This method captures the coupled three dimensional effects of wing geometry parameters. Using this method, a large set of basis data was generated by varying wing thickness, aspect ratio, taper ratio, and sweep angle for a trapezoidal wing with a symmetric NACA 00XX airfoil section. From this basis data, meta-model equations were created for form factor and critical Mach number as functions of thickness, aspect ratio, taper ratio, and sweep angle.

Since this previous work utilized a symmetric airfoil section, the coupled effects of various possible camber lines and thickness forms were not included. Furthermore, the correlation to a desired design lift coefficient or angle of attack was not included in the formulation of the form factor and critical Mach number meta-model equations.

The motivation for this paper was to develop a design methodology for allocating wing thickness that includes the effects of airfoil camber lines and thickness forms, while also considering the design lift coefficient for the wing section. The goal was to apply the previously developed method for calculating

critical Mach number from pressure coefficients to various popular airfoil sections in order to investigate the effects on the critical Mach number of camber lines and thickness forms at various lift coefficients or angles of attack. From this investigation a method for allocating wing thickness and camber as a function of desired critical Mach number and section lift coefficient will be developed for each airfoil type. This method can then be applied along with the previously developed method to capture the effects on critical Mach number from an airfoil camber line and thickness form as well as a wing thickness, aspect ratio, taper ratio, and sweep angle.

II. Critical Mach Number for Cambered Thick Wing Sections and Finite Wings

To develop a method for calculating critical Mach number the wing geometry parameters of interest must first be defined. Next, a method for calculating critical Mach number and drag divergence Mach number must be chosen for this study. A review of past work in this field as well as other methods for estimating critical Mach number will be presented. From this, the objectives and goals for the development of a new method for calculating critical Mach number as a function of certain wing geometry parameters will be outlined.

A. Wing Geometry and Critical Mach Number

A trapezoidal wing can be defined by three nondimensional parameters and one dimensional parameter – thickness ratio, aspect ratio, taper ratio, and leading edge sweep angle. With the planform of the wing defined, the cross sections need to be considered next. The airfoil cross sections of a wing can be defined nondimensionally by a mean camber line and a thickness form. This mean camber line is typically defined for a reference "airfoil design lift coefficient." For certain airfoils, this can be scaled simply by multiplying the mean camber line by the ratio of the desired airfoil design lift coefficient and the original airfoil design lift coefficient. For certain other airfoils, this does not apply, and the mean camber line must be looked up from a database for each airfoil design lift coefficient that is to be considered. The thickness form, on the other hand, can simply be scaled by the desired maximum thickness ratio for any given airfoil section.

The critical Mach number for some given wing configuration is defined as the freestream Mach number at which some point on the wing reaches a local Mach number of one. The critical Mach number, M_{cr}, can be calculated directly from fluid dynamics relations. The critical pressure coefficient, C_P^*, where the flow first goes supersonic, is related to the freestream Mach number as in Eq. (1)[2].

$$C_p* = \frac{2}{\gamma M_{cr}{}^2}\left\{\left[\frac{2+(\gamma-1)M_{cr}{}^2}{(\gamma+1)}\right]^{\frac{\gamma}{(\gamma-1)}} - 1\right\} \tag{1}$$

If the pressure distribution for a wing section defined by the parameters discussed above is known, then a minimum pressure coefficient for that section can be extracted. Using the above Eq. (1), and setting the minimum pressure coefficient as the critical pressure coefficient ($C_P^* = C_{P_{\min}}$), the critical Mach number of a wing section can be computed. This method of using pressure coefficients obtained from low Mach number testing, or zero Mach number computations, to calculate a critical Mach number was developed by von Karman and used to build the data presented in *A Summary of Airfoil Data*, NACA Report 824[3].

It is also convenient to define a drag divergence Mach number, M_{DD}. For the two-dimensional airfoil section, NACA Report 832[4] defines drag divergence as the speed at which $\frac{\partial C_D}{\partial M} = 0.10$. This is a parameter commonly used in aircraft design. It relates to the critical Mach number, yet provides a bit more insight into the transonic performance characteristics of an aircraft since it is directly correlated to the wing section drag characteristics.

B. Past Works and Studies of Cambered Thick Wing Sections

Several other works in the past have studied the effects of wing and airfoil geometry parameters on critical Mach number. Some of the most popular of these are reviewed here to aid in establishing a study technique and development of a new method. Also, there are several common methods used to estimate critical Mach number. These are reviewed here to describe viable methods for estimating critical Mach number, but also to point out certain limitations of these methods, which have provided further motivation to develop a new method for estimating critical Mach number.

An important primary source is NACA Technical Report 832, *A Systematic Investigation of Pressure Distributions at High Speeds Over Five Representative NACA Low-Drag and Conventional Airfoil Sections*[4]. Several models of two dimensional wing sections were tested in a wind tunnel. The airfoils for these wing sections included the symmetric NACA 00XX series, the NACA 65 series, the NACA 230 series, as well as some others. The report includes pressure distributions for these airfoils as well as plots comparing trends of critical Mach number at various section lift coefficients for these airfoils. This report is a great resource for wind tunnel data for these given airfoils, however, the electronic copy available from NASA is not of high quality and it can be quite difficult to extract data points from some of the plots.

NACA Technical Report 824, *A Summary of Airfoil Data*[3], is another source of aerodynamics data for various airfoil sections. The work from this report has also been included in *Theory of Wing Sections*[5]. A much broader set of airfoils is covered in these two references. *Theory of Wing Sections* also includes the details of the airfoils' geometries including things like surface ordinates, mean camber lines, and thickness forms. The two dimensional data presented includes lift curves, drag polars, and also plots of critical Mach number as a function of section lift coefficient. This is another important source for wind tunnel data as well as airfoil geometry descriptions and general airfoil theory and design.

From surveying the above references a few key points were observed to setup and guide this study. First, the above testing was done on two dimensional wing sections for the various airfoils. This is obviously appropriate for obtaining things like pressure distributions and lift curves. However, it is interesting that testing done to examine critical Mach number has historically been done with two dimensional wing sections. Of course, simple sweep theory can be applied to account for the effects of sweep angle, but this does not account for any other three dimensional effects of wing geometry parameters, such as those discussed in *Zero Lift Drag and Drag Divergence Prediction for Finite Wings in Aircraft Design*[1]. This suggests that the effects of the airfoil sections of a wing on critical Mach number can be superpositioned with the effects of the planform geometry of the wing.

This aligns well with the authors' philosophy that for allocation purposes, the geometric characteristics of a wing that affect critical Mach number can be separated into two parts. The first is the planform geometry of the wing that consists of an average thickness ratio, aspect ratio, taper ratio, and leading edge sweep angle. The second is the geometry of the airfoil sections of the wing, which is described by a mean camber line and a thickness form. These two parts of the overall wing's geometry can be combined in a superposition method to fully address their effects on the critical Mach number of the wing.

Also, the plots shown in the above references of critical Mach number versus section lift coefficient show some interesting trends that suggest a relatively simple relation that can possibly be described by some functional relation. This will be discussed further in the section below in relation to existing methods.

C. Existing Methods for Estimating Critical Mach Number

There are a few methods for estimating critical Mach number which are commonly used in aircraft design. These methods are reviewed in detail in *Zero Lift Drag and Drag Divergence Prediction for Finite Wings in Aircraft Design*[1], and a brief overview is provided here to discuss the techniques used as well as some of their appropriate ranges of applicability. These provided insight into possible techniques to be used in developing a new method, but also provided the motivation to develop a new method with a broader range of applicability.

The Empirical Drag Estimation Technique (EDET)[6] is the basis of the aerodynamics analysis used within the NASA FLOPS sizing code. Based on a user input of a maximum airfoil thickness, a maximum percent camber, a selection of either a "conventional" or "advanced airfoil," and a maximum operating Mach number, EDET performs an empirical analysis to estimate a design Mach number about which lift dependent drag rise tables are pivoted. This empirical analysis is based on a large set of aerodynamic performance data for various subsonic and supersonic aircraft. Although EDET's empirical analysis has proven to work quite well, it is formulated as an analysis method and cannot be used for inverse design to allocate a spanwise distribution of wing thickness.

The Stability and Control DATCOM[7] book set is an aerodynamics data compilation developed for and maintained by the United States Air Force. The DATCOM method graphically interpolates amongst an experimental data set of wing sections to estimate a critical Mach number or drag divergence Mach number. This empirical analysis is based on wing thickness, aspect ratio, and freestream Mach number. The experimental basis data for this analysis consists of testing done on wing sections with NACA 6-series airfoils at various aspect ratios and Mach numbers. This basis data is very limited in its applicable range of airfoil section. Furthermore, DATCOM also provides an analysis method and not a design method that can be used to inverse design a spanwise allocation of wing thickness.

The Korn Equation is another method used to estimate critical Mach number. The Korn Equation[8], Eq. (2), is a simplified empirical relation that describes the dependence between critical Mach number, airfoil thickness, the section lift coefficient of an airfoil section, and a technology factor, *k*.

$$M_{cr} = \mathrm{k} - 0.1C_{l_{section}} - t/c \tag{2}$$

The exact history of the development of the Korn equation is not well documented. However, what is most important is that it provides some functional relation between critical Mach number, section thickness and design lift coefficient. This relation was more than likely created based on some experimental and/or computational data for critical Mach number as a function of section lift coefficient for various thickness ratios. Recall the discussion of the plots shown in NACA Technical Report 832 and 824. The Korn equation seems to define this very functional relation that was discussed. This functional relation provides a design method that can be used to inverse design a wing thickness simply by solving the equation for the thickness term.

Furthermore, the Korn Equation includes the parameters of interest for describing the effects of an airfoil section's geometry on critical Mach number. The effects of the mean camber line are captured by the section lift coefficient term and the effects of the thickness form are captured by the thickness term. However, a scaling of these effects is also necessary to make the simple functional relation applicable to various airfoils. This is achieved through the airfoil technology factor.

Although the Korn equation works quite well for various airfoils, the technology factor term creates a shortcoming of the equation. To obtain a correct technology factor for an airfoil section, a set of experimental or computational data of critical Mach number as a function of section lift coefficient for various thicknesses must be acquired. This in itself may not necessarily be difficult for certain popular airfoils, and even for certain unconventional airfoils it can be obtained somewhat easily. However, the shortfall lies in the applicability of the overall functional relation of the Korn Equation. Although the above mentioned data sets may be available, the functional relation itself may not necessarily apply to all airfoil sections. The relation is really only applicable to the airfoils used in the original data sets used to create the equation. This may work well for certain other airfoil sections, but there are many airfoil sections for which the Korn Equation does not produce accurate results.

Nevertheless, the technique or method used to create the Korn Equation is very applicable to the efforts of this paper and it provided the main inspiration to develop a new method for estimating a critical Mach number for a given airfoil section with a defined camber line and thickness form that will be applicable to a broader range of airfoil sections.

D. Motivation and Goals For New Method Development

The main motivation to develop a new method to calculate a critical Mach number for a given airfoil section was three fold. First, the trends demonstrated in past experiments and studies along with the existence of the Korn Equation suggested that some functional relation could potentially be drawn between the critical Mach number, thickness form, and mean camber line of an airfoil section. Second, while a method had been developed to capture the three dimensional effects of wing thickness, aspect ratio, taper ratio, and sweep angle on critical Mach number[1], a method was needed to also capture the effects of the camber lines and thickness forms of the wing sections. Third, a method was needed that would apply to a very broad range of airfoil types and that could be used as an inverse design method in the realm of a set of multidisciplinary aircraft design tools and processes.

As discussed earlier, it was evident from past work and existing methods that two dimensional airfoil data obtained from testing or computation could be used to investigate the relation between critical Mach number and the section lift coefficient for an airfoil with varied thickness. This technique can be combined with the method used to compute critical Mach number from the pressure distributions along a wing section, as described above in Section II.A. This is also the method used in *Zero Lift Drag and Drag Divergence Prediction for Finite Wings in Aircraft Design*[1].

First, a detailed investigation of various airfoil sections needs to be conducted. Parameters such as lift coefficient, pressure distributions, and critical Mach number must be examined for various airfoil shapes having different mean camber lines and thickness forms. Based on these observations, a method can be developed to somehow relate critical Mach number with the geometric characteristics of an airfoil section.

Recall that the main purpose of this new method is for it to be used amongst a set of multidisciplinary aircraft design tools and processes for advanced conceptual and preliminary design. This developed relation must be general enough to apply to several different airfoil sections or possibly families of similar airfoil sections. If this is not achievable with acceptable accuracy, it may only be specific and applicable to certain airfoils. In which case, the method needs to be easily and rapidly repeatable so that a relation can be created for any type of airfoil that the aircraft designer is interested in studying. In particular, the designer must be able to apply the method to unconventional and revolutionary shapes for advanced aircraft studies. The method must also be a design method so that the designer can use it as an inverse design tool to allocate wing thickness and camber. And lastly, it must be simple to code, run quickly, and integrate well with other tools and methods.

III. Investigation of the Effects of Camber and Thickness on Critical Mach Number

A. Introduction

With the above motivations to develop a new method for calculating critical Mach number for a given airfoil geometry, a detailed examination of the performance of a few select airfoils of differing types will be conducted. First, some general two dimensional airfoil characteristics will be compared with reference data to validate the study process and tools. Along with this, variations in the airfoil parameters will be tested to verify they exhibit some of the expected effects. Next, a large set of data, acquired through a semi-automated computation process, will be used to observe trends and relations of critical Mach number as a function of various airfoil geometry and performance parameters. The observations from these trends in this data will be the basis for developing the new method.

B. Implementation

Three airfoils were selected for this investigation. They were chosen to be popular airfoils used in various aircraft configurations with significant reference data available, yet are all different types of airfoils. These were selected to be studied in the initial investigation to demonstrate the capability to develop a new method for estimating critical Mach number for these types of airfoil sections. Future work will expand the studies to a broader set of airfoils, yet the development method should remain the same.

The three airfoils chosen were a NACA 65 series airfoil, a NACA 230 series airfoil, and a supercritical SC(2) series airfoil. Figure 1 below displays each of these airfoils along with its respective thickness form, camber form, and chordwise pressure distribution shape.

The NACA 65 series is a popular series of airfoils used on various existing aircraft. This series is considered to be a laminar flow series of airfoils characterized by an extended chordwise region of a favorable pressure gradient. However, they are and have been used on wing designs that are not necessarily designed to fly with a significant portion of laminar flow along the wing. The NACA 65 series has a simple thickness form similar to that of the symmetric NACA series of airfoils, except the maximum thickness location is shifted to the chordwise center of the airfoil section. The mean camber line for the NACA 65 series is also simple and parabolic with the maximum camber location also being at the chordwise center of the airfoil section. The design lift coefficient for the NACA 65 series mean camber line is 0.75. As described in Section II.A., the camber lines for this series of airfoils can be easily scaled by multiplying the mean camber line by the ratio of the desired design lift coefficient to the original design lift coefficient[5].

The NACA 230 series of airfoils are most popularly known for their "peaky" pressure distributions. The term "peaky" refers to the fact that the pressure distribution "peaks" in the forward section of the airfoil, around 10% or 20% of the chord from the leading edge of the airfoil, and then falls off sharply. This characteristic of the pressure distribution will result in a shockwave forming at about 20% to 30% of the chord from the leading edge of a wing section. The thickness form of the NACA 230 series is also a simple thickness form similar to that of the NACA symmetric series, but the maximum thickness point is near the 30% chord location. The mean camber line for this series shows that the maximum camber is at the 15% chord location and does not vary much until aft of the 30% chord location where it drops off quickly to zero. The NACA 230 series mean camber line is given for an airfoil design lift coefficient of 0.30, and this can be scaled similar to the NACA 65 series[5].

The supercritical SC(2) series of airfoils is the second generation of supercritical airfoils that are commonly used for transonic aircraft. These airfoils have a pressure distribution that rises sharply at the leading edge and maintains a nearly constant pressure coefficient, which then drops off sharply near or aft of the 50% chord location. This characteristic of the pressure distribution places a shockwave at the aft end of the wing section. The thickness form for the supercritical series of airfoils is similar to that of the NACA 65 series near the leading edge with a portion near the mid section that maintains a flat thickness form. The thickness form then drops off and is near zero for a portion of the trailing edge. The camber line for the supercritical series features little or no camber in the forward half of the airfoil, and a parabolic positive camber in the aft end of the airfoil. The mean camber line for the supercritical series of airfoils cannot be scaled as easily as the NACA 65 or 230 series. Hence, for each airfoil design lift coefficient, a mean camber line was extracted from surface ordinate data[9].

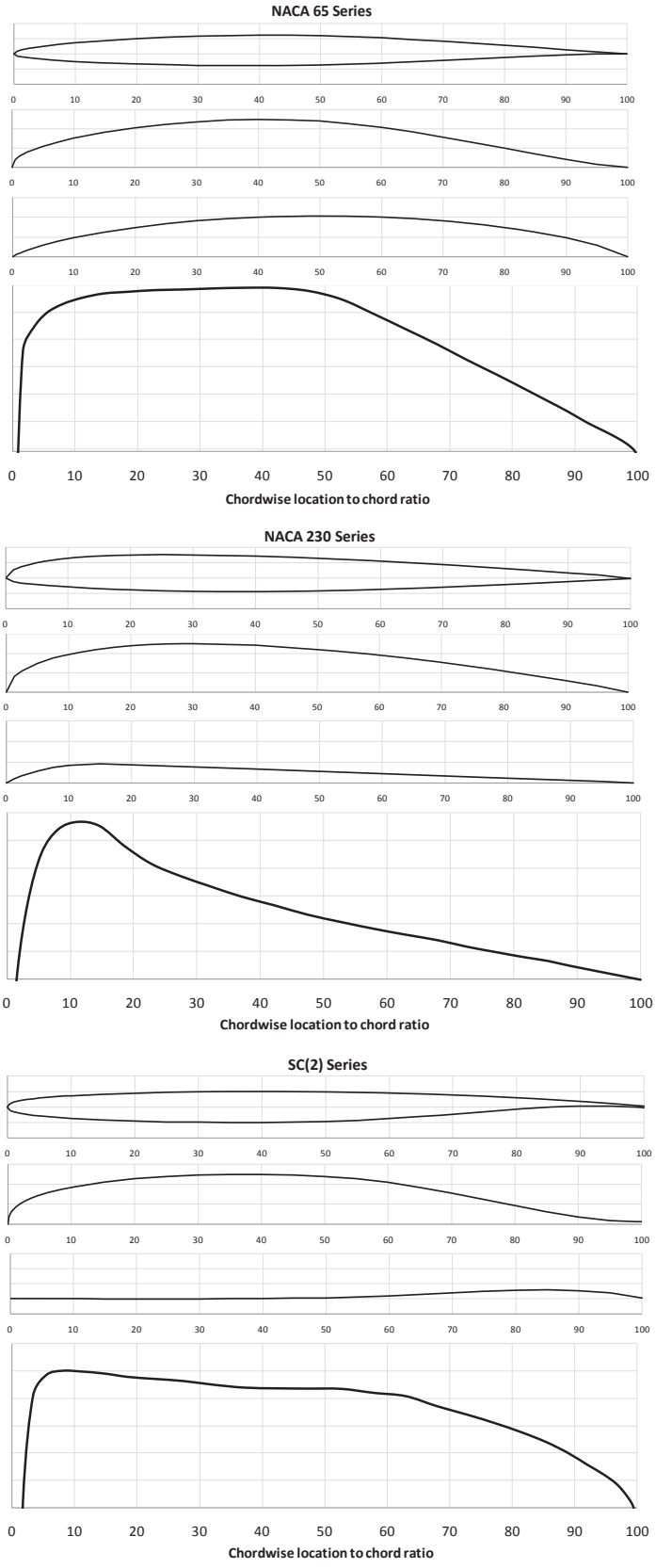

Figure 1. Airfoil shape, thickness form, mean camber line, and pressure distribution shape for NACA 65 Series, NACA 230 series, and supercritical SC(2) series airfoils[5,9].

These three airfoils were analyzed using the three dimensional potential flow code, VORLAX. The thick, cambered, sandwich panel element formulation was implemented in VORLAX by modeling an upper surface and a lower surface of the wing. This sandwich panel model allows thickness to be accurately modeled in a vortex lattice method. The models were analyzed at a Mach number of zero to model only subsonic conditions. Verification of the results from the sandwich panel modeling methods of VORLAX is presented in *Zero Lift Drag and Drag Divergence Prediction for Finite Wings in Aircraft Design*[1]. Recall that the objectives for this study were to examine the critical Mach number characteristics of two dimensional wing sections. To do so, while utilizing the preferred potential flow methods of VORLAX, a three dimensional wing section with a large aspect ratio, no taper, and no sweep was used for the computational wing model. An aspect ratio trade was performed to verify that minimal or no three dimensional effects were present in the model. This trade is shown in Fig. 2 below. At aspect ratios of about 50 and greater, the pressure distributions for the wing section are nearly the same. Hence, an aspect ratio of 50 was used for this study.

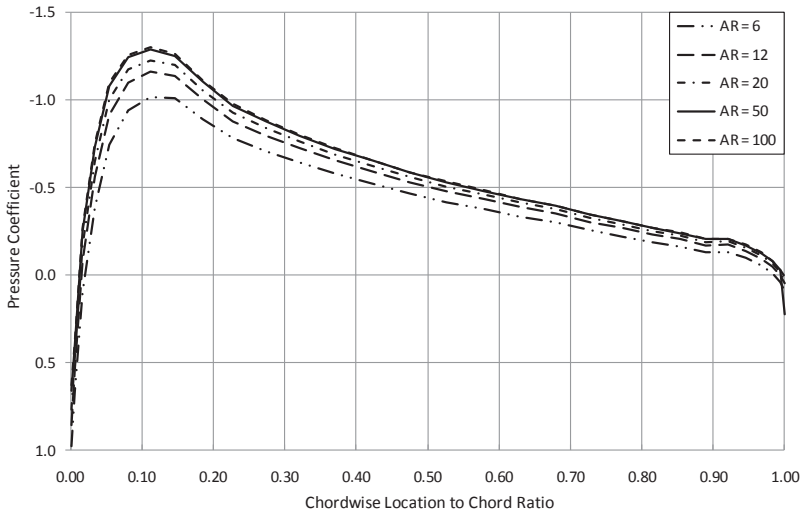

Figure 2. Effects of AR on a NACA 230 Series airfoil wing.

Another reason for using VORLAX was that it integrated well with the methods developed by the team to calculate a critical Mach number for a wing section from its chordwise pressure coefficients. This method calculates a critical Mach number from direct theoretical fluid dynamics relations and the pressure coefficients of the wing section include any and all effects of the wing section geometry.

An automated process was established to run VORLAX for various wing section thicknesses and various airfoil design lift coefficients or camber scalings, as described earlier. The test matrix of cases analyzed is shown below in Table 1. For each case a section lift coefficient, critical Mach number, and the location of the minimum pressure coefficient were computed at each angle of attack. For certain other cases, the lift curve and section pressure distribution were also examined. These encompass the parameters of interest required to observe the critical Mach number characteristics of these airfoils.

	Thickness to Chord Ratio	Percent Camber	Angle of Attack
NACA 65 Series	0.06, 0.08, 0.10, 0.12, 0.15, 0.18, 0.21	0%, 27%, 53%, 80%, 100%	-8˚ to 8˚
NACA 230 Series	0.06, 0.08, 0.10, 0.12, 0.15, 0.18, 0.21, 0.24	0%, 50%, 100%, 150%, 200%	-8˚ to 8˚
Supercritical SC(2)	0.06, 0.08, 0.10, 0.12, 0.15, 0.18, 0.21	0%, 100%, 125%, 150%, 175%, 250%	-8˚ to 8˚

Table 1. Matrix of airfoil sections analyzed.

As described above, the data acquisition portion of this study was automated, wherever possible, to fulfill the test matrix shown in Table 1. Before performing the data acquisition, verification exercises where performed to ensure that the scaling methods, discussed earlier, being used in the automated process were correctly modeling the airfoils outlined in the above test matrix. Figure 3 below shows a sample of a thickness scaling verification for a set of NACA 230 series airfoils, while Fig. 4 shows a sample camber scaling verification for a set of NACA 65 series airfoils. These scaling methods used in the automated modeling reproduce the airfoil ordinates properly. For the supercritical family of airfoils, each set of ordinates was manually inputted.

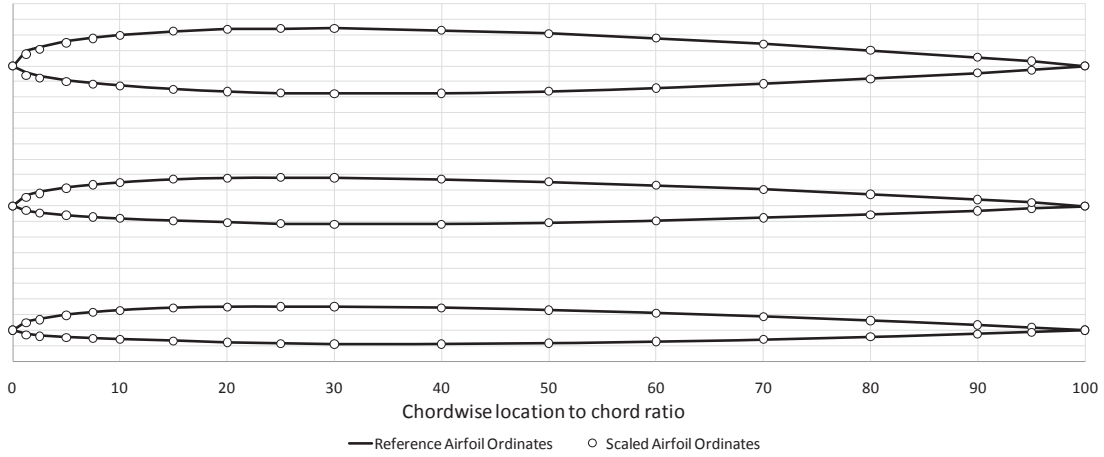

Figure 3. Verification of thickness scaling method for a set of NACA 230 series airfoils[5].

Figure 4. Verification of camber scaling method for a set of NACA 65 series airfoils[5].

C. Investigation Results

For the purposes of developing a method to allocate wing section thickness and camber, the most important trends to observe are those of critical Mach number as a function of section lift coefficient as thickness and camber are varied for a given airfoil family. A portion of the data collected from the matrix in Table 1 above is displayed in this section in order to observe some interesting trends in the performance of the three studied airfoil families. In all cases, the lack of smoothness in the curves is a result of computational tolerances.

Figures 5-7 show critical Mach number variations with thickness for the three families of airfoils, each at its design camber case. First, it is interesting to note that for each airfoil family, the lines are centered near the airfoil design lift coefficient for the given percent camber condition. Each family of airfoils possesses a sort of useful range near the center of the curves, outside of which the critical Mach number drops drastically. As thickness is increased, the lines decrease in their values of critical Mach number and the useful range of the lines is widened. Also note that the NACA 65 and 230 series airfoils have a

characteristic plateau shape in their lines, while the supercritical airfoils maintain a sort of peak that slightly flattens as thickness is increased.

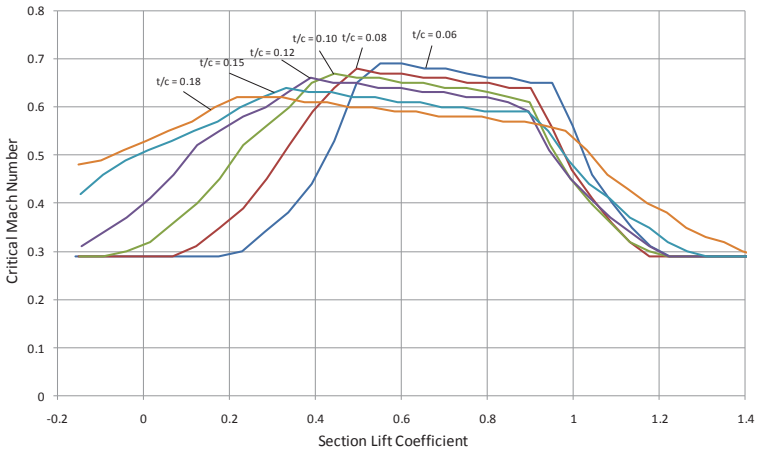

Figure 5. Critical Mach Number vs. Section Lift Coefficient for varied thicknesses of a NACA 65 series airfoil at its design camber.

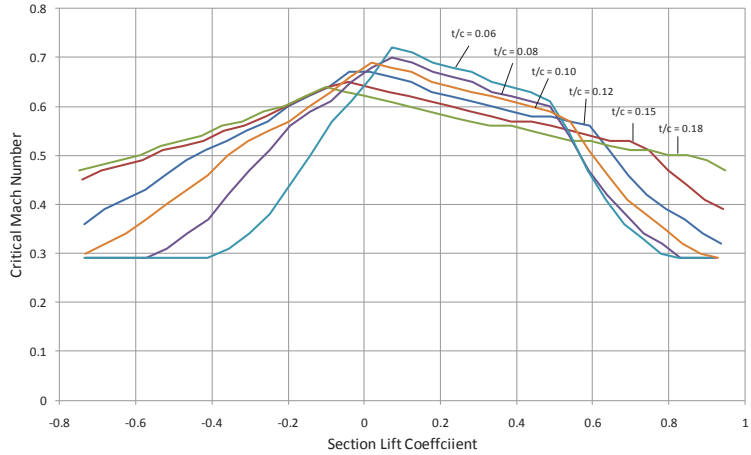

Figure 6. Critical Mach Number vs. Section Lift Coefficient for varied thicknesses of a NACA 230 series airfoil at its design camber.

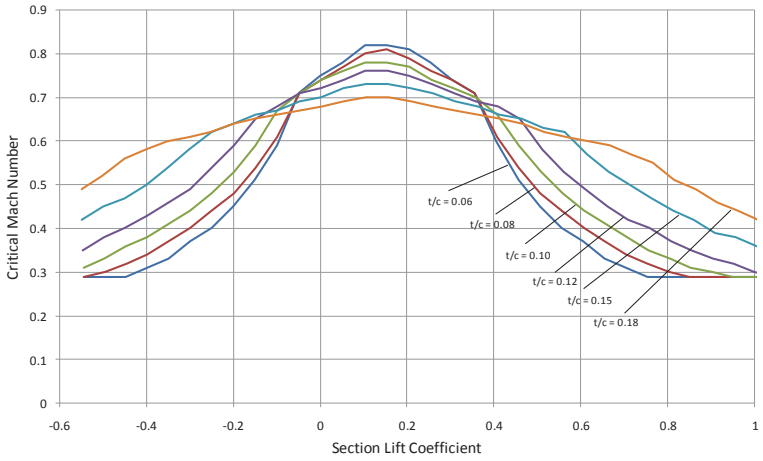

Figure 7. Critical Mach Number vs. Section Lift Coefficient for varied thicknesses of a SC(2) series airfoil at its design camber.

Figures 8-10 show critical Mach number variations with camber for the three families of airfoils, each at a thickness to chord ratio of 0.10. These plots further demonstrate how the lines tend to be centered near the airfoil's design lift coefficient, with the zero percent camber cases demonstrating this best. Furthermore, as camber is increased, the lines shift to the right along the section lift coefficient axis. The NACA series of airfoils tend to decrease in overall critical Mach number as the camber is increased, while the supercritical series decrease very little in critical Mach number as the camber is increased.

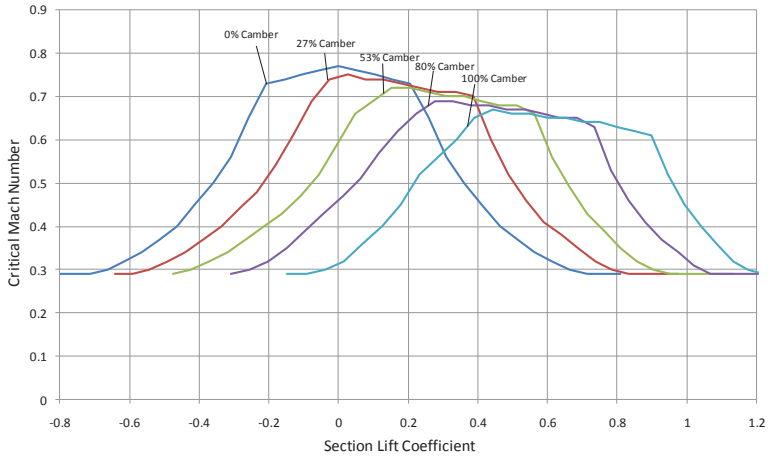

Figure 8. Critical Mach Number vs. Section Lift Coefficient for varied camber of a NACA 65 series airfoil at a thickness to chord ratio of 0.10.

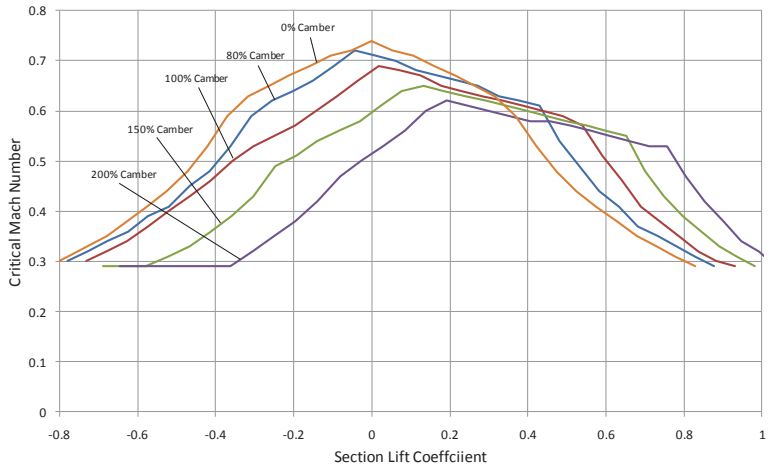

Figure 9. Critical Mach Number vs. Section Lift Coefficient for varied camber of a NACA 230 series airfoil at a thickness to chord ratio of 0.10.

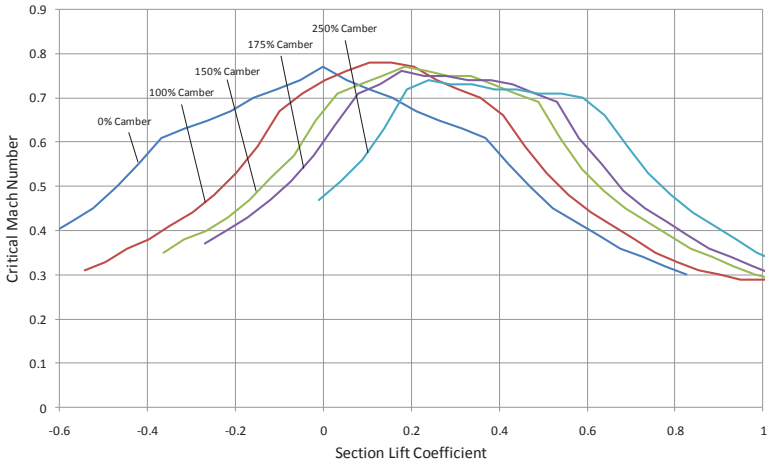

Figure 10. Critical Mach Number vs. Section Lift Coefficient for varied camber of a SC(2) series airfoil at a thickness to chord ratio of 0.10.

Figure 11 below shows variations in both thickness and in camber for the NACA 65 series airfoil. Three thickness ratios at three different percent cambers are plotted in this figure. Lines of the same color have the same percent camber.

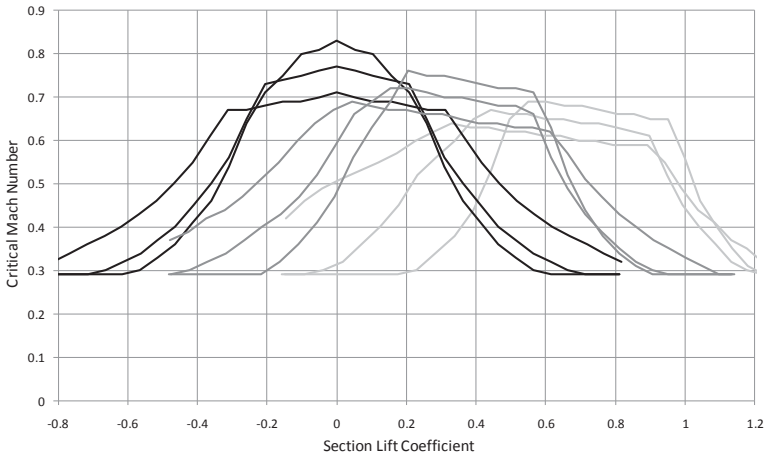

Figure 11. Critical Mach Number vs. Section Lift Coefficient for three thickness ratios at three different percent cambers for the NACA 65 series. *Lines of the same color have the same percent camber and vary in thickness.*

Including any additional thickness ratio or percent camber cases in Fig. 11 above makes the plot difficult to view. Nevertheless, this figure serves to demonstrate the possible combinations of thickness ratio and percent camber that populate the design space of coupled critical Mach numbers and section lift coefficients.

D. Discussion of Results

The plots shown in Fig. 5-11 depict behaviors of the various families of airfoils in terms of section lift coefficient and critical Mach number as thickness ratio and percent camber are varied. In increasing thickness, the reduced capability in terms of critical Mach number is expected, since this acts to increase relative velocities along the airfoil section, which in turn reduce the critical Mach number. Increasing camber can have a similar effect, yet not in exactly the same manner since increasing camber may not affect the relative velocities as much as an increase in thickness. Increasing the camber also shifts the above curves to higher section lift coefficients, as is expected.

These observations along with the depiction of the critical Mach number and section lift coefficient design space in Fig. 11 comprise the challenges of the engineer's task in allocating wing section thickness and camber to achieve a desired critical Mach number and section lift coefficient. Imagining the design space filled with all possible thickness ratios and percent cambers further exemplifies the difficultly of performing such a task manually. Aside from the large amounts of computation time that are involved in analyzing this data, there may be several different combinations of thickness ratio and percent camber that achieve the desired critical Mach number and section lift coefficient. Hence, the designer must use the analysis data above and apply some sort of trade study or optimization to select the proper combination of thickness ratio and percent camber for a given airfoil family. Such a process was considered and incorporated into the development of a new method.

IV. Development of a New Method for Allocating Wing Thickness and Camber

The above investigation of the trends in critical Mach number and section lift coefficient for varied thickness to chord ratios and percent cambers for each family of airfoils provides the insight necessary to develop a design method for allocating wing thickness and camber. As discussed earlier, for a desired critical Mach number and a required section lift coefficient, a pairing of thickness to chord ratio and percent camber can be selected from the above set of data. However, recreating this analysis process for each design iteration for each given aircraft configuration is quite tedious and time consuming. An automated method that maintains an equivalent level of fidelity and uses the same theoretical methods is desired to improve the capabilities of the design engineer. The NACA 65 family of airfoils was selected to

demonstrate the development of such a method for this paper. However, the process is designed to be rapidly repeatable and applicable to any and all airfoil shapes.

A. Theoretical Background

The goal of this work is to develop an airfoil section design method in which the designer specifies a minimum required critical Mach number (M_{cr}) and a corresponding minimum required section lift coefficient (C_l). The method then calculates the corresponding "optimized" airfoil section geometry that maximizes thickness-to-chord ratio (t/c) and minimizes the airfoil design lift coefficient ($C_{ldesign}$), or percent camber.

The utility of this method is twofold. Firstly, it greatly reduces the dimensionality of the design problem: the designer may specify M_{cr} and $C_{ldesign}$, two degrees of freedom, and use the method to produce an approximately 100-degree of freedom airfoil loft. Secondly, it is more efficient for the designer to specify desired performance metrics and directly solve for the geometry than it is to specify the geometry and solve for the corresponding performance metrics, iterating until the desired performance is achieved.

It is instructive to distinguish between "forward" and "inverse" design. Figure 12 illustrates a forward airfoil design process ("loft and analyze"), in which the analysis code takes in an airfoil geometry and flow conditions and outputs the section M_{cr} and C_l. The design process requires successive analysis iterations, driven using an optimizer, until the "best" values for M_{cr} and C_l are found. The bottom process in Fig. 12 illustrates the same problem being solved using an inverse design process. Here the designer specifies M_{cr} and C_l and the inverted analysis (Geometry Solver) determines an airfoil geometry and flow (in this case, angle of attack) that yields the specified M_{cr} and C_l.

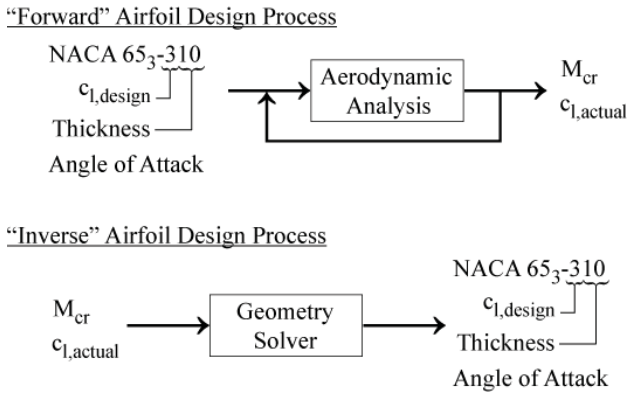

Figure 12. Comparison of information flow for forward and inverse design processes.

We call the coordinate space spanned by the variables on the left of the Aerodynamic Analysis in Fig. 12, and their associated allowable or feasible ranges, the "design space," and the corresponding mapping of this space in the variables on the right of the Aerodynamic Analysis the "response space." In the remainder of this section, these terms will be used in a general sense to refer to the corresponding concepts for notional design problems with arbitrary numbers of design variables and response metrics and an arbitrary (forward) design analysis.

Conditions for Invertibility

In order for a functional design analysis to be invertible, there must be a one-to-one relationship between its design space and its response space. For deterministic analysis codes, the mapping from the design space to the response space is always unique. For the analysis code to be invertible, however, there must also be a unique mapping from the response space back to the design space. This type of relationship between the analysis's inputs and outputs is properly called a bijection.

Most design analyses are not naturally bijections for the simple reason that there are typically more design variables than response metrics, and the design variables are usually independent. Because the

design variables are independent, each represents a "degree of freedom" for the problem. Thus, we have more degrees of freedom than dimensions of the response space. For a design analysis with n design variables and $m<n$ response metrics, this usually implies that a particular set of values for the output metrics does not correspond to a unique set of values for the n design variables, but to an m-n dimensional manifold in the design-variable space.

Simply matching the number of input variables and output variables (i.e. $n=m$) does not guarantee a bijective relationship. The functional relationship between the inputs and outputs must also be *monotonic*. While monotonicity is easily demonstrated for univariate functions, it can be difficult to visualize for high-dimensional functions. An equivalent, more tractable, condition is that none of the response metrics may have a minimum or maximum value except at the boundaries of the design space.

Strategy for Developing an Inverse Design Methodology

How, then, can a general design analysis, with arbitrary numbers of design variables and response metrics, whose relation may be non-monotonic, be inverted? Our strategy is to invert the analysis code only over a lower-dimensional manifold (i.e. a subset of the design space) that meets the following two conditions:

1. The manifold has the same dimensionality in the design space and the response space.
2. The mapping from the manifold in the design space to the response is monotonic.

Note that Condition 2 is intended to constrain the choice of the manifold rather than the choice of the design analysis, which we presume is predetermined and not subject to modification.

While these two conditions are sufficient to ensure the analysis code is invertible over the specified manifold, two additional conditions are needed to ensure the resulting inverted analysis is useful as a design tool:

3. Except for the possibility of a (small) finite number of discontinuities, the manifold is continuous in both the design space and the response space.
4. The manifold contains all of the designs that are "good."

Condition 3 requires that the inverted analysis be able to perform meaningful parametric sensitivity studies. Essentially this condition requires that two designs that are within a small neighborhood of the response space are usually within a small neighborhood in the design-variable space. The disclaimer "except for a finite number of discontinuities" implies that such a neighborhood does not have to exist in all directions around a given design; rather at a given design, the manifold, viewed in the design space, is continuous in at least one direction. As it turns out, the airfoil design problem considered here has no discontinuities, so we will not consider this condition further.

Condition 4, intends to ensure that every design that is in some sense "optimal" can be returned by the inverted analysis. This condition arises from the logical presumption that the designer will request "good" designs from the inverted analysis, and so we must ensure that these designs are included in the invertible manifold. We will define "good" and "bad" designs more formally below.

At a glance, it appears that finding a manifold that meets the above four conditions will be difficult – perhaps more difficult than iterating the normal forward design process to convergence. It turns out, however, that a manifold that meets the above conditions exists for general design problems, and moreover the manifold coincides with a well-studied subset of the response space: the Pareto frontier.

This is the realization that enabled the present inverse design methodology. The Pareto frontier, which can be found by using a multi-objective optimizer, is an invertible subset of the design space that includes all "good" designs. We can now formally define a "good" design as one that is non-dominated. A non-dominated design is formally defined as one that cannot be improved in one objective without degrading at least one other objective. Hence, our claim that the Pareto frontier satisfies Condition 4 is based on the premise that decision makers will always prefer a non-dominated design to a dominated design. This is not

to say that every non-dominated design is "good," but rather that, assuming all response metrics of interest are being considered, a rational decision maker will always prefer a non-dominated design to a dominated one. Although not a focus of this paper, it is additionally worth noting here that discontinuities as mentioned in Condition 3 above can arise in problems for which the "global" Pareto frontier contains intersections of multiple "local" Pareto frontiers.

Our investigations suggest that the Pareto frontier inverse design method described here is applicable to a large class of problems in which the mapping from the design space to the response space is continuous. However, we do not attempt to rigorously demonstrate the method's generalizibility in this in this paper. Instead, we will simply demonstrate post facto that the Pareto frontier of the particular airfoil design problem being considered here satisfies the Conditions for invertibility outlined above. In the following section, we describe our inverse design methodology and its application to the present problem in greater detail.

B. Application of Inverse Design Methodology to Airfoil Design

Figure 13 shows the steps in the design analysis inversion methodology. The two main requirements are to find the Pareto frontier of the forward design analysis and then to create a model of the Pareto frontier that is useful as an inverse design tool. For the present problem, these requirements were accomplished using the processes described in the corresponding boxes in Fig. 13. Each step in these processes is described below.

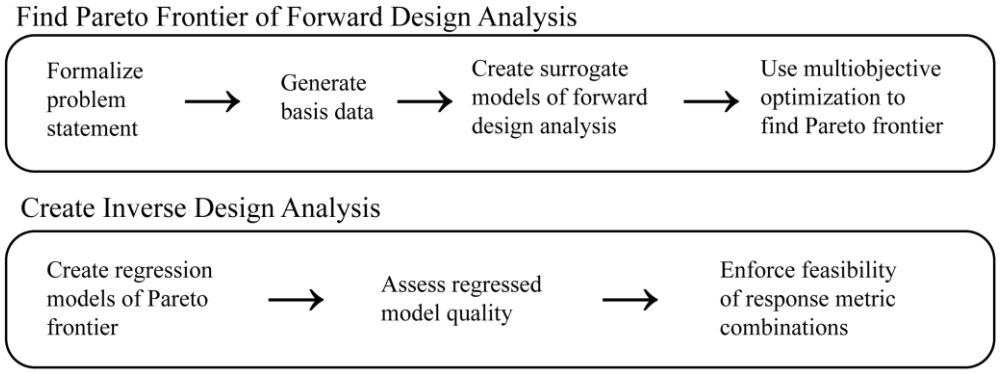

Figure 13. Steps for creating inverse design analysis

Formalize Problem Statement

The methodology begins by formally defining the desired inverse design formulation. In the present problem, the goal is to create an inverse design method in which the designer specifies the desired Mcr and the desired C_l, and the inverse design analysis returns the maximum allowable t/c and $C_{ldesign}$ (for a NACA 65-series airfoil) to achieve the specified M_{cr} and C_l, as well as the corresponding angle of attack. Though the method is extensible to multiple airfoil families, consideration is limited here to the NACA 65-series. In addition to establishing the variables of interest, bounds on the variables must be decided on in order to limit the scope of the problem to interesting designs. In the present work, we bound the design space by placing upper and lower limits on the t/c, $C_{ldesign}$, and angle of attack values considered. The bounds on these variables are chosen based on experience to represent the space of designs that are relevant to some notional design problem. These choices imply corresponding limits for the values of M_{cr} and C_l that may be specified as inputs to the inverse design analysis. The limits of all variables as considered in this study are shown in Table 2.

Limit	Thickness/Chord	$C_{l,design}$	Angle of Attack	M_{cr}	C_l
Lower	0.01	0.0	-8°	0.944	-0.856
Upper	0.20	0.8	8°	0.299*	1.482

*constrained by limits of forward design analysis code

Table 2. Design variable and response metric limits.

Depending on the nature of the forward design analysis code, it may be possible to run a multi-objective optimizer directly on the design analysis code. In the present work, we instead create surrogate models of the forward design analysis code and use the surrogate models in the multi-objective optimization.

Create Surrogate Models for M_{cr} and C_l

The relationship between the airfoil geometry and the aerodynamic response metrics is continuous, but is not smooth. In particular, the relationship between angle of attack and M_{cr} has several kinks, visible in Fig. 5, whose location and severity depends on the airfoil's thickness and camber.

The presence of these kinks makes fitting a surrogate model difficult, as many types of models will smooth out the kinks, resulting in an inaccurate model. Because these surrogate models are only intermediate steps to creating the final inverted model, we chose to utilize a simple linear interpolation between a dense grid of basis data. This technique requires running a larger number of cases using the actual analysis code than might be needed for a particular strategically chosen surrogate model form. However, the number of cases required for this problem was not impractical and the linear interpolation method is suitable for the purposes of demonstrating the creation of the inverse design analysis.

Find the Pareto Frontier using Multi-objective Optimizer

In this study, Pareto frontiers were found using the NSGA-II algorithm[10]. Recall that the goal of the multiobjective optimizer is to obtain a (smooth) invertible manifold. This requires a densely populated, highly converged optimization. Consequently, care must be taken to ensure that the multi-objective optimizer has converged to the true Pareto frontier. This is often difficult to determine by looking at the resulting values of the objective functions, but can be judged by looking for a lack of numerical noise in the corresponding values of any (non-objective) variables that are inputs to the objective functions. Ensuring such convergence may require a larger optimizer population size than is typically used for other optimization applications. This underscores the need for fast surrogate models that can be used by the optimizer in place of the original design analysis.

In order to ensure that the inverse design analysis can produce any design that might be considered "good," the Pareto frontier must be calculated over all objectives regardless of whether they comprise design variables or response metrics. Thus, for the present problem, the preliminary multi-objective function considered was $max(M_{cr}), max(t/c), max(C_l), min(C_{ldesign})$.

A cross-sectional slice of the Pareto frontier corresponding to this multi-objective function is illustrated in Fig. 14a. In most places, the frontier is essentially a two-dimensional surface (hence the slice in Fig. 14a is nearly one-dimensional in most places), while at certain combinations of low t/c, high C_l, and high $C_{ldesign}$ the frontier becomes three-dimensional (two-dimensional in Fig. 14a).

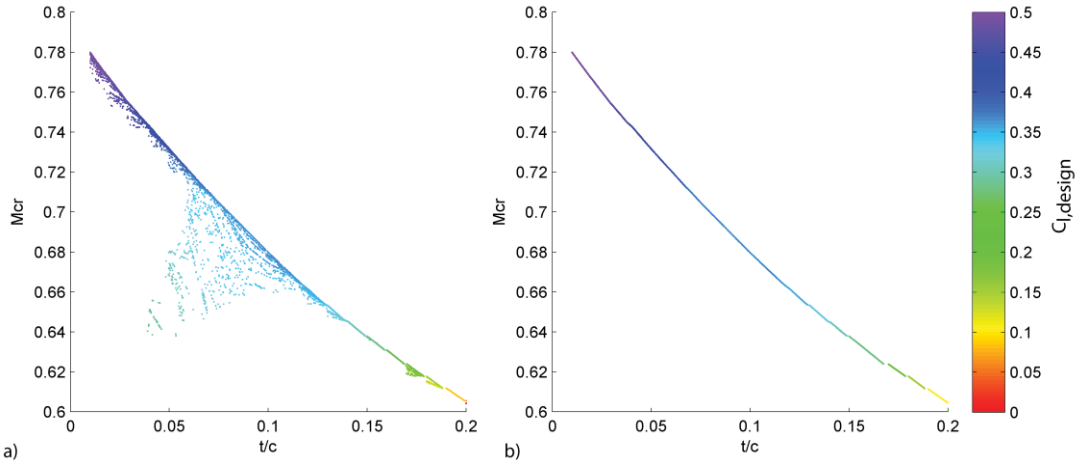

Figure 14. Cross-section view of Pareto frontiers at C_l=0.5 *a) Pareto Frontier of max(M_{cr}), max(t/c), max(C_l), min($C_{ldesign}$); b) Pareto frontier of max(M_{cr}), max(t/c), max(C_l)*

The emergence of the third dimension corresponds to the region where it is possible to trade off t/c and $C_{ldesign}$ to maintain a constant level of C_l and M_{cr}. This is clearly seen in Fig. 14a – C_l is constant for all points in this graph, and Mcr is constant along any horizontal line. In regions where such a line crosses multiple points, it is possible to freely choose t/c within some range. In other regions, t/c and $C_{ldesign}$ trend favorably such that the thickest, least cambered design is always preferred.

Because this Pareto frontier has three dimensions, the corresponding inverse design problem would require three independent variables. The most useful formulation for such a problem seems to be to consider M_{cr}, C_l and "preference for maximizing t/c vs. minimizing $C_{ldesign}$" as the independent variables and t/c and $C_{ldesign}$ as the dependent variables. However, this formulation is somewhat awkward in its use of a "preference" variable whose value has no effect over a large portion of the design space – the regions where the Pareto frontier is two-dimensional.

In order to simplify the inverse problem formulation, we add the additional constraint "given the choice between a thicker airfoil and an airfoil with lower $C_{ldesign}$, always choose the thicker airfoil." This constraint seems reasonable considering the "steepness" of the required tradeoff, which, as seen in Fig. 14a, requires that a large amount of thickness must be given up for only a small improvement in $C_{ldesign}$. Implementing this constraint is equivalent to removing $C_{ldesign}$ as an objective while calculating the Pareto frontier. Consequently, the final multi-objective function used in this study was *max(M_{cr}), max(t/c), max(C_l).*

A cross-section slice of the resulting three-objective Pareto frontier is illustrated in Fig. 14b, and the full frontier is illustrated in Fig. 15. Notice that Fig. 14b is exactly the upper limit of the point set in Fig. 14a. The three-objective frontier is two-dimensional everywhere (one-dimensional in any C_l=constant slice, as in Fig. 14b), hence the inverse design problem will require two independent variables, which we choose to be M_{cr} and C_l. It is worth noting that the choice of which two variables to treat as independent is not constrained by our previous classification of variables as design variables or response metrics. For example, an alternate formulation could use M_{cr} and t/c as the independent variables. Furthermore, we note that the Pareto frontier, as shown in Fig. 15 is monotonic; thus it satisfies our conditions for an invertible manifold for creating an inverse design analysis.

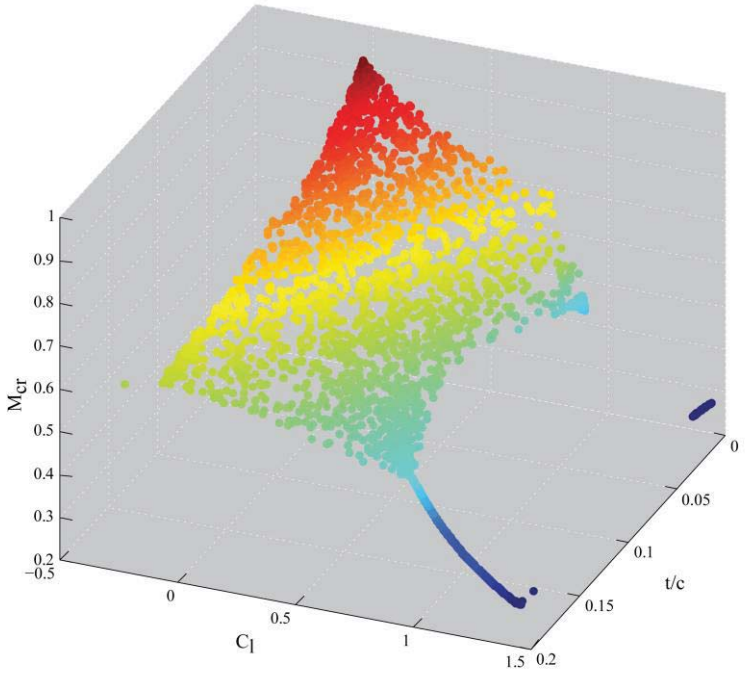

Figure 15. Sampled three-objective Pareto frontier of max(M_{cr}), max(t/c), max(C_l). *Found using NSGA-II optimizer. Point color corresponds to M_{cr} axis.*

Before proceeding to create inverse analysis models, one additional simplification was made. The Pareto frontier, as shown in Fig. 15, contains designs with negative C_l and designs that have low Mcr with high C_l. We reason that these designs are not "good" and we remove them from consideration by enforcing the additional constraints $0 < C_l < 0.8$. (Recall the previous explanation that the Pareto frontier contains all "good" designs, but not all designs on the Pareto frontier are "good.") This constraint could alternately have been enforced during the multi-objective optimization itself. The inclusion of these limits on C_l is not strictly necessary to create a working inverse design tool, but it simplifies the functional form of the models creates in the next steps.

Create Inverse Models

The inverse design problem formulation requires the creation of two models: t/c as a function of M_{cr} and C_l; and $C_{ldesign}$ as a function of M_{cr} and C_l. In our formulation, t/c and $C_{ldesign}$ are each modeled separately using an artificial neural network. Note that although neural networks were found to be unable to accurately model the kinks of the original forward design analysis, the final Pareto frontier does not have kinks (after removing the high C_l designs) and consequently good fits can be obtained by using neural nets.

The relationship between t/c, M_{cr} and C_l is rather simple, and an excellent model was. The relationship between $C_{ldesign}$, M_{cr}, and C_l is more complex. Despite imposing the limits on C_l, a discontinuity in the smoothness of the $C_{ldesign}$ function still exists. This can be clearly seen in Fig. 16, and is due to the fact that in this formulation we do not allow $C_{ldesign}$ to be negative, i.e. by allowing the airfoil to be upside down, although the trend seen in Fig. 16 suggests that in some cases this would be preferred. Consequently, our forward design analysis returns $C_{ldesign} = 0$ over a large portion of the space. We fit $C_{ldesign}$ using a piecewise neural network, as shown in the equation below. The third order polynomial in the "if" statement corresponds to the boundary of the $C_{ldesign} = 0$ region.

Figure 16 shows the inverse design equations evaluated over the interval $0 < C_l < 0.8$, $0.55 < M_{cr} < 0.95$. Because of the bounds on t/c that are implicit in the problem formulation, the entirety of this interval is not feasible. In particular, the region outside of the black curves corresponds to values of t/c outside of those considered in the initial forward analysis. Hence, the neural networks may be highly inaccurate in these regions and should not be used, even if such values of t/c are deemed appropriate.

The final inverse analysis equations for the NACA 65-series are:

$$
\begin{aligned}
&C_{l,design} = \\
&\textbf{if } 6.5359 - 19.415044*M_{cr} + 19.58818*M_{cr}^{2} - 6.7322*M_{cr}^{3} - C_l < 0 \\
&\quad (-4.244712 \\
&\quad - 3.864341 * logsig(-26.119837 + 36.769728*M_{cr} + 3.974681*C_l) \\
&\quad + 6.321264 * logsig(12.389707 - 13.943638*M_{cr} - 0.788833*C_l) \\
&\quad - 5.435434 * logsig(16.362991 - 18.327723*M_{cr} - 5.453603*C_l) \\
&\quad + 6.156389 * logsig(-25.558023 + 35.219003*M_{cr} + 7.776769*C_l) \\
&\quad) * 0.204578 + 0.310564 \\
&\textbf{else} \\
&\quad 0
\end{aligned}
\tag{3}
$$

$$
\begin{aligned}
&t/c = \\
&(0.110230 \\
&+ 2.817773 * logsig(10.128619 - 14.200437*M_{cr} - 0.136473*C_l) \\
&+ 2.973346 * logsig(6.355732 - 6.515870*M_{cr} - 3.899726*C_l) \\
&- 3.337924 * logsig(-16.208464 + 27.629532*M_{cr} + 1.000548*C_l) \\
&) * 0.058187 + 0.095356
\end{aligned}
\tag{4}
$$

$$
\textbf{logsig(x)} = 1 / (1 + exp(-x)) \tag{5}
$$

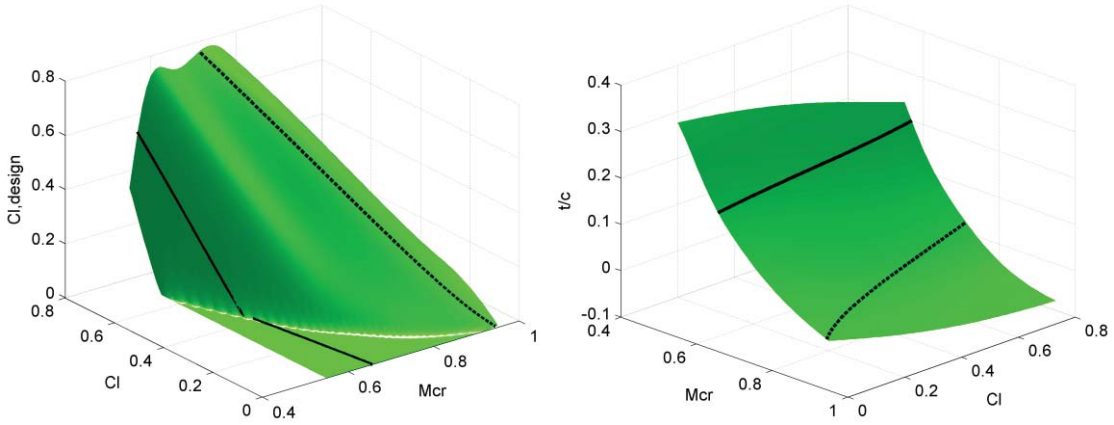

Figure 16. Surface plots of inverse design neural networks. *Equations are valid over the range of M_{cr}, C_l between the black curves. The solid curve corresponds to t/c=0.2 and the dashed curves corresponds to t/c=0.01.*

An assessment of the neural network's error distributions is presented in Fig. 17 and 18. The fit of t/c is excellent, due to the lack of noise in the multi-objective optimization results and the simplicity of the mapping from Mcr and Cl to t/c (as seen in Fig. 16). The fit of $C_{ldesign}$ is less good. Although this may seem to be due to the complexity of the mapping from Mcr and Cl to $C_{ldesign}$ (as seen in Fig. 16), the poorness of fit is actually due to numerical noise in the optimization results on which the fit is based. Recall that the final objective function used was *max(M_{cr}), max(t/c), max(C_l).* This function does not include $C_{ldesign}$, and so the optimizer itself was essentially unaware that $C_{ldesign}$ even existed as a metric. Instead, the values of $C_{ldesign}$ are simply calculated as a post-processing step for the designs composing the Pareto frontier found by the optimizer. While this strategy generally works well to obtain a low-noise manifold in metrics of interest that are not directly included in the Pareto frontier, there is an additional complication in the present problem: the similarity between the effects of $C_{ldesign}$ and angle of attack.

Simply put, $C_{ldesign}$ (a measure of camber) and angle of attack have very similar effects on C_l and M_{cr}. The multiobjective optimizer is essentially unaware of these variables, and has no way of resolving this similarity. Rather, we rely on the fact that the two effects are not *exactly* the same and thus a (noiseless)

$C_{ldesign}$ manifold should theoretically exist. The results seen in Fig. 17, however, show that we have not exactly found this manifold. Furthermore, we note that the inversion techniques described here will generally fail when two design variables exist that have identical effects on the response metrics. Further work is needed to determine how best to enhance this method to account for such situations.

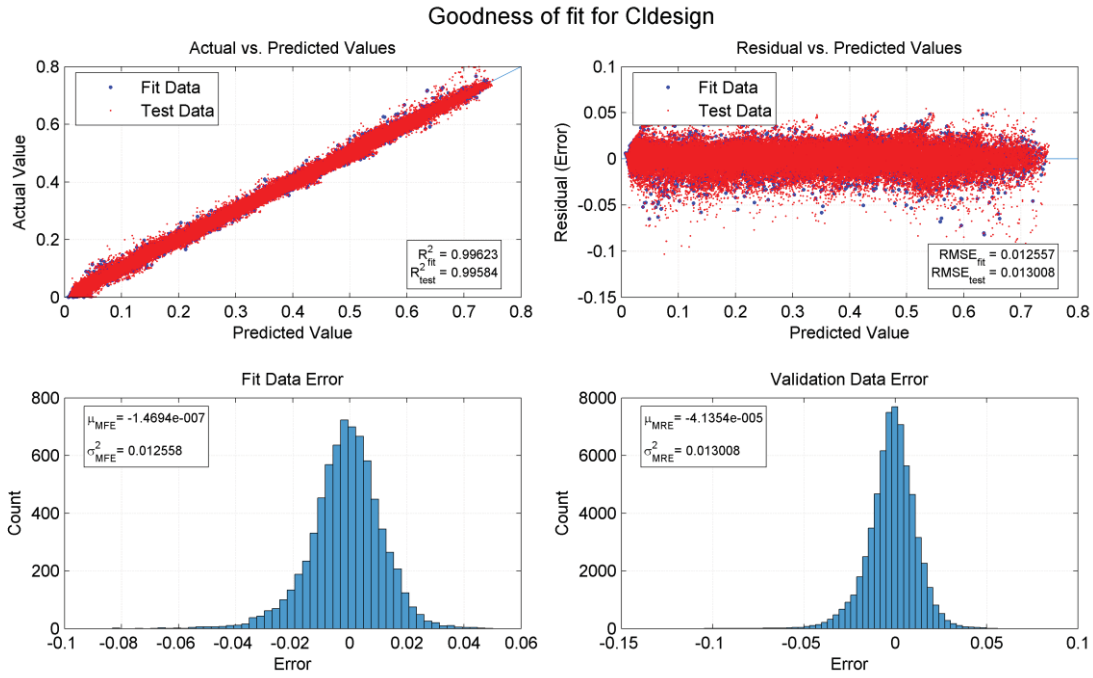

Figure 17. Summary of $C_{ldesign}$ inverse design neural network quality

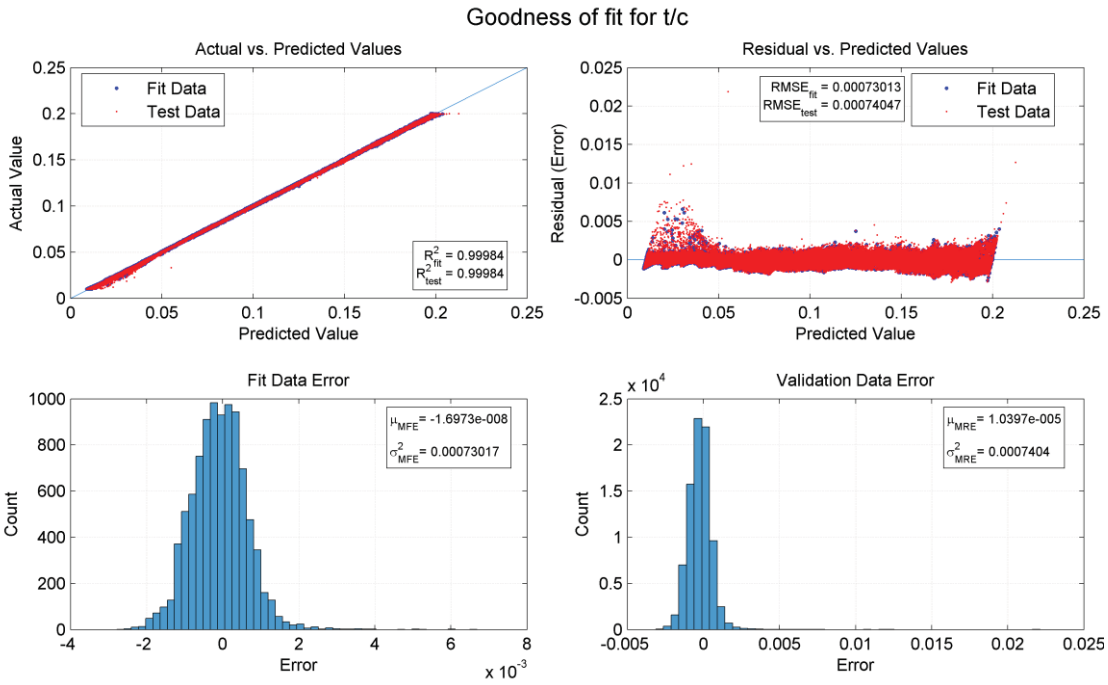

Figure 18. Summary of t/c inverse design neural network quality

Enforce Feasibility of M_{cr}/C_l combinations

There remains a rather significant hurdle to implementing the inverse design technique described here for general, high-dimensional design problems. The response metrics of any design problem are generally not independent, and consequently it is impossible to create an (inverse) design method that lets the designer independently specify values for each response metric. Given such freedom for a general high-dimensional problem, it is exceedingly likely that the designer would specify a combination of response metrics for which no corresponding design exists. In this case, additional steps would be needed to guide the designer in choosing feasible combinations of the response metrics.

For the present problem, however, the dimensionality of the Pareto frontier is sufficiently low that simple graphical aids are sufficient to inform the designer of the allowable combinations of response metric values, thus avoiding the need for more complicated decision making aids. In Fig. 19 a plot of the projection of the inverse design manifold (Pareto frontier) into the M_{cr} vs C_l plane clearly shows the limits of the designs that can be analyzed using the inverse design model created here. Note that these limits correspond exactly to the constraints already specified: the ranges listed in Table 2 and the constraint that $0 < C_l < 0.8$. It may be helpful to re-express these constraints as functions of M_{cr} and $C_{ldesign}$, since those are now considered to be the independent variables. For the present problem, these constraints are:

t/c < 0.2 constraint:

$$C_l - (8.0887 - 15.3404*M_{cr} + 7.1734*M_{cr}^2) < 0$$

t/c > 0.01 constraint:

$$(0.2177 + 9.7874*M_{cr} - 15.4074*M_{cr}^2) - C_l < 0$$

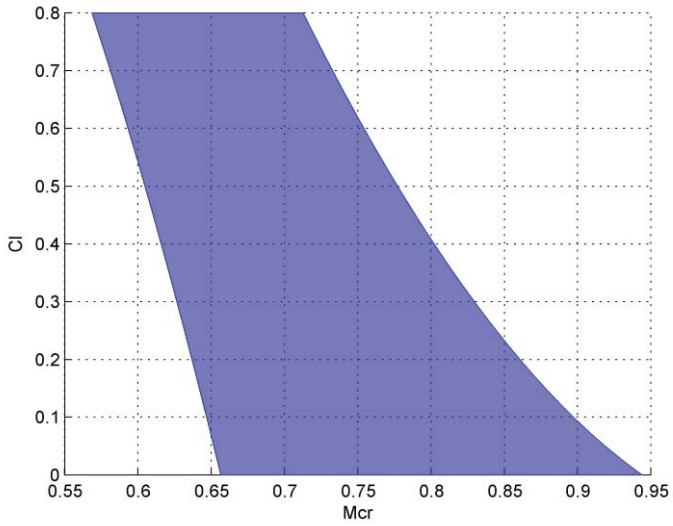

Figure 19. Locus of allowable combinations of M_{cr}, C_l (shaded) for use with inverse design neural networks. *Combinations outside of this region have t/c<0.01 (at right) or t/c>0.2 (at left)*

V. Conclusions

The challenges of properly allocating wing section thickness and camber for a given wing configuration based on a desired critical Mach number and section lift coefficient provided the initial motivation to develop an improved method for allocating thickness and camber. Traditional methods and past works suggested that the development of such a method was possible. A detailed analysis investigation of three different families of airfoils and the effects of thickness ratio and percent camber on their critical Mach numbers and section lift coefficients provided the insight into the design space required to formulate a new method to allocate thickness and camber.

The analysis data for the investigation was gathered using a vortex lattice method coupled with fundamental fluid dynamics. Hence, these data sets include the combined effects of the airfoil geometry's thickness and camber and avoid the use of any empiricism. Furthermore, these data sets can be generated relatively quickly and easily for any chosen family of airfoils.

The additional realization that the Pareto frontier of the airfoil design space is an invertible manifold provided the key to creating a rapid, non-iterative method for allocating thickness and camber based on desired critical Mach number and section lift coefficient. A multi-objective optimizer was used to interpolate the vortex lattice basis data to find the Pareto frontier. The Pareto frontier was then fit using two neural networks to calculate thickness and camber as a function of critical Mach number and section lift coefficient. The resulting neural networks can be used as inverse design tools to allocate thickness and camber.

This new inverse design method for allocating wing thickness and camber provides the design engineer increased capability and fidelity in designing a wing for a given aircraft. Furthermore, it allows the design engineer to avoid using an analysis method to allocate thickness and camber, or any method involving some level of empiricism. The method development process itself can be performed rapidly and can be applied to any family of traditional or custom airfoils, allowing the designer to implement such a design tool across a much broader range of applicability.

References

1. Takahashi, T.T., German, B., Shajanian, A., Daskilewicz, M., Donovan, S., "Zero Lift Drag and Drag Divergence Prediction for Finite Wings in Aircraft Design," AIAA 2010-846.
2. Anderson, J., *Introduction to Flight*, McGraw Hill, Boston, 2000.
3. Abbott, I.H., Von Doenhoff, A.E., Stivers, L, "Summary of Airfoil Data," NACA Report 824, 1945, pp. 270.
4. Graham, D.J., Nitzberg, G.E., and Olson, R.N., "A Systematic Investigation of Pressure Distributions at High Speeds Over Five Representative NACA Low-Drag and Conventional Airfoil Sections," NACA Report 832, 1945.
5. Abbott, I.H., Von Doenhoff, A.E., Stivers, L, *Theory of Wing Sections*, Dover Publications, 1959.
6. Feagin, R. C., and Morrison,W. D., "Delta Method, An Empirical Drag Buildup Technique," Lockheed-California Co., Rept. LR-27975-VOL-1, 1978.
7. Fink, R.D., Hoak, D.E., "USAF Stability and Control DATCOM," McDonnell Douglas Corporation Douglas Aircraft Division, Project No. 8219, October 1960.
8. Mason, W.H, *Virginia Tech Configuration Aerodynamics Class Notes*, http://www.aoe.vt.edu/~mason/Mason_f/ConfigAero.htm (retrieved Feb 15, 2009).
9. Harris, C.D., "NASA Supercritical Airfoils – A Matrix of Family-Related Airfoils," NASA Technical Paper 2969, March 1990.
10. Deb, K.; Pratap, A.; Agarwal, S. & Meyarivan, T. "A fast and elitist multiobjective genetic algorithm: NSGA-II," IEEE Transactions on Evolutionary Computation, 2002, 6, 182 – 197.